

Table I. Gases in which stimulated thermal Rayleigh scattering was investigated. Frequency shifts, thresholds, and critical absorption coefficients α_{cr} are given.

Gases	Density (amagat)	α (cm^{-1})	Anti-Stokes shift (cm^{-1})		Threshold (MW)	α_{cr} (cm^{-1})	
			Calc.	Obs.		Calc.	Obs.
CO ₂ +NO ₂	71	0.025	0.013	0.012	3.2	0.012	a
N ₂ +NO ₂	47	0.007	0.013	0.008	10	0.0069	0.007
He+NO ₂	47	0.050	0.013	STRS not observed		0.0018	a
N ₂ +I ₂	47	0.060	0.013	0.004	<6	0.0069	<0.05

^aNo stimulated Brillouin scattering observed.

A similar result was obtained when iodine crystals were placed in the gas cell with N₂ gas at 47 amagat. At room temperature with input power of 30 MW, the back-scattered light corresponded to the Brillouin shift. As the temperature was raised the Brillouin gradually weakened and disappeared at 95°C, $\alpha=0.02 \text{ cm}^{-1}$. At 115°C, the I₂ absorption was great enough ($\alpha=0.05 \text{ cm}^{-1}$) to produce STRS.

The above results are summarized in Table I. The calculated values of α_{cr} were obtained from Eq. (3), assuming complete thermalization and using available material parameters.⁵ It was also assumed that $(\Gamma_L + \Gamma_R)/(\Gamma_L + \Gamma_B) = 1$ in gases. STRS was sought in He with NO₂ for absorptions up to 0.056 cm^{-1} . None was seen for input powers up to 60 MW, presumably because of the small value of α_{mol} .

The authors wish to thank Dr. A. H. Guenther of the Weapons Laboratory, Kirtland Air Force Base, for the use of the giant-pulse laser sys-

tem, and R. M. Herman and M. A. Gray of this department for numerous helpful discussions.

*Work supported by the U. S. Office of Naval Research and the National Science Foundation.

†On leave from Memorial University of Newfoundland, St. John's, Newfoundland, Canada.

¹R. M. Herman and M. A. Gray, Phys. Rev. Letters **19**, 824 (1967).

²D. H. Rank, C. W. Cho, N. D. Foltz, and T. A. Wiggins, Phys. Rev. Letters **19**, 828 (1967).

³G. I. Zaitsev, Yu. I. Kyzylasov, V. S. Starunov, and I. L. Fabelinskii, Zh. Eksperim. i Teor. Fiz.—Pis'ma Redakt. **6**, 802 (1967) [translation: JETP Letters **6**, 255 (1967)].

⁴F. Gires and G. Mayer, Compt. Rend. **266B**, 8 (1968).

⁵International Critical Tables (McGraw-Hill Book Company, Inc., New York, 1930); Handbook of Chemistry and Physics, edited by C. D. Hodgman (Chemical Rubber Publishing Company, Cleveland, Ohio, 1967); D. H. Rank, T. A. Wiggins, R. V. Wick, D. P. Eastman, and A. H. Guenther, J. Opt. Soc. Am. **56**, 174 (1966).

KAPITZA EFFECT IN GASEOUS HELIUM*

C. F. Mate and S. P. Sawyer

Department of Physics, Ohio State University, Columbus, Ohio

(Received 27 December 1967)

An adequate account of the thermal boundary resistance between solids and liquid helium II, first observed by Kapitza,¹ has not yet been found either by extension^{2,3} of Khalatnikov's⁴ discussion or by the consideration of a variety of heat-transfer mechanisms.⁵ Apparently, discussion of the Kapitza effect requires a new point of departure. Here we report some measurements relevant to the suggestion that the kinetics of adsorbed helium atoms play an important part in heat transfer between helium and a solid boundary.⁵ If this is so, the

Kapitza resistance should not depend greatly on the density, or for that matter the phase, of the bulk helium.

We have investigated the heat transfer between helium gas and a copper surface at low temperatures. In order to be able to distinguish between surface resistances and bulk resistive effects, we constructed a conductance cell in which the width of the sample space is very small, nominally 10μ . The cell, shown in Fig. 1, consisted of two oxygen-free, high-conductivity copper cylinders (2 cm diam) mount-

ed with their end faces parallel in a thin-walled cupro-nickel tube. Alignment and spacing of the cell faces was accomplished during assembly of the cell by placing a 0.25-mil Mylar spacer between them. The cell faces had been polished smooth, but not flat, to 0.1μ , each being left with a convex profile which could be approximated by $\gamma = 1.6 \times 10^{-4} r^2$ cm as determined by interferometric comparison with an optical flat. The measurements of cell conductance were corrected for the radial variation of gap width, and for the change in width produced by differential thermal contraction when the cell was cooled.

During the conductance measurements, cell-face temperatures were determined from the readings of the carbon resistance thermometers T_3 and T_4 , corrected for temperature gradients in the copper. The thermal resistivity of the copper was measured *in situ* with a second pair (T_1, T_2) of resistance thermometers. The cell was enclosed in a vacuum jacket immersed in a liquid-helium bath. The bottom of the vacuum jacket was used as heat sink for the cell. An additional thermometer (T_5)

was the sensor for a temperature regulator, which, using the heater and the thermal stand-off at the lower end of the cell, performed the important function of decoupling the cell from temperature fluctuations in the helium bath.

Figure 2 shows our measurements of cell conductance, as a function of temperature, at eight different gas (^4He) pressures ranging from 0.1 to 350 mm Hg. The measurements extend down to the saturation temperature for each pressure. Within the scatter of the data there is no irregularity in the temperature dependence at the lambda point.

Neglecting edge effects, the thermal resistance of the cell can be written as the sum of three terms,

$$R(\text{cell}) = R(\text{gas}) + 2R(\text{Knudsen}) + 2R(\text{Kapitza}), \quad (1)$$

if it is assumed that at each cell face there is a gas-kinetic temperature jump introducing a resistance $R(\text{Knudsen})$ between the bulk gas and a layer of adsorbed helium. $R(\text{Kapitza})$ is then the boundary resistance between the adsorbed layer and the copper surface. Kinetic theory gives, per unit area of the surface,

$$R(\text{Knudsen}) = g/k,$$

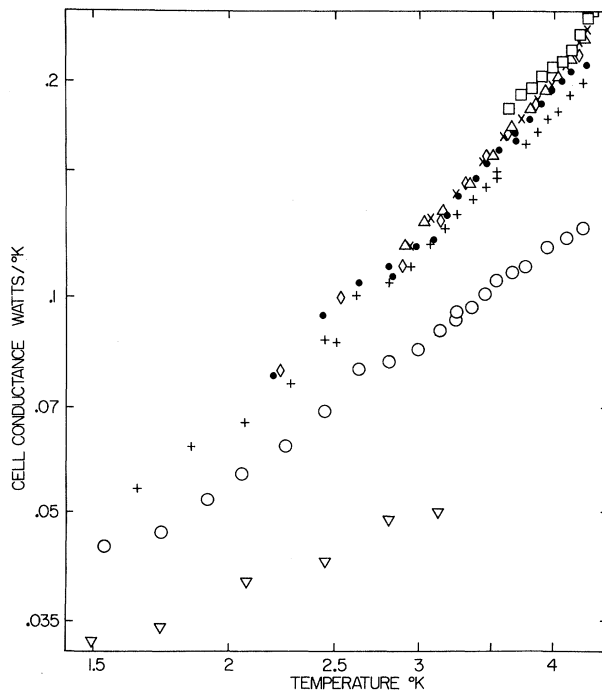
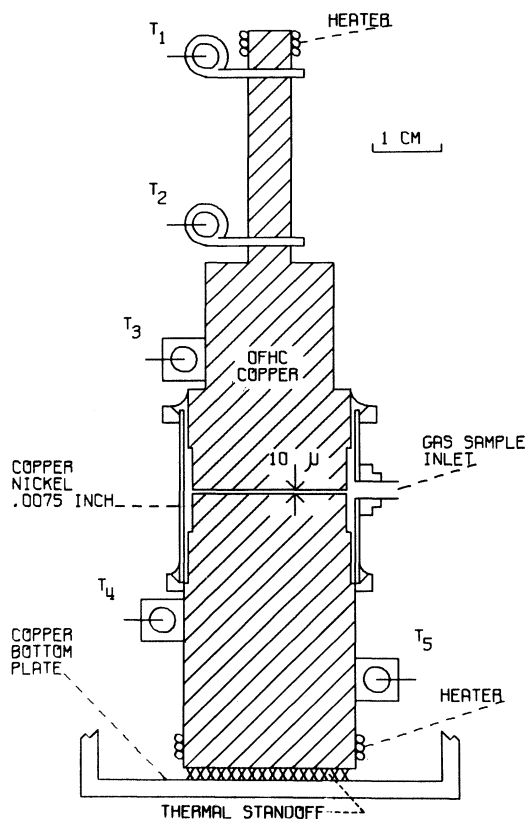


FIG. 2. Cell conductance at eight different ^4He gas pressures. See Fig. 3 for legend.

where κ is the conductivity of the bulk gas, and⁶

$$g = \frac{2-\alpha}{\alpha} \frac{(\gamma-1)}{(\gamma+1)} \frac{\kappa}{P} \left(\frac{2\pi T}{R} \right)^{1/2}, \quad (2)$$

in which α is the accommodation coefficient, R is the gas constant (per gram), γ is the ratio of gaseous specific heats, P is the pressure, and T is the temperature of the gas at the wall. Since g varies inversely as the pressure, R (Knudsen) vanishes at sufficiently high pressures. In Fig. 2, the downward displacement of the cell conductance curves for the three lowest pressures displays the increasing dominance of the Knudsen effect as the mean free path in the gas becomes comparable with the cell width. To correct for the Knudsen effect in the low-pressure data we chose a value for α in Eq. (2) that removed the pressure dependence from the data. The value thus obtained for the accommodation coefficient was $\alpha = 0.72$. As might be expected with a value near unity, there was no detectable variation of α with temperature.

After correcting for the Knudsen effect, which in any case is negligible at the higher pressures, we found that the thermal resistance of the cell could not be accounted for in terms of the resistivity of the bulk gas.⁷ There was always a positive residue which we have taken the liberty of attributing to a "gaseous" (actually, "adsorbed-layer") Kapitza effect. The Kapitza resistance computed for each datum point in Fig. 2 is shown in Fig. 3. The appearance of this pressure-independent resistive term is our justification for using Eq. (1) to describe the heat-transfer processes in the conductance cell.

With a cell width of 10μ , the surface and bulk-gas contributions to the cell resistance are comparable. For instance, at 1.5°K , $R(\text{gas}) = 33.5^\circ\text{K}/\text{W}$, while $R(\text{Kapitza}) = 31.1^\circ\text{K}/\text{W}$ for 1 cm^2 of cell surface area. The corresponding resistances at 4.0°K are 11.9 and $4.4^\circ\text{K}/\text{W}$. Over the same temperature range, $R(\text{Knudsen})$ increases from $2.25P$ to $3.7P \text{ cm}^2^\circ\text{K}/\text{W}$, where P is in mm Hg.

The precision of the data in Fig. 3 is probably not as good as might be inferred from the scatter of the points. An error of $\pm 2 \mu$ in the estimated cell width is possible, and would give an error of $\pm 40\%$ in the boundary resistance at the middle of the temperature range. However, the boundary resistance cannot be made to vanish by a revision of the estimated

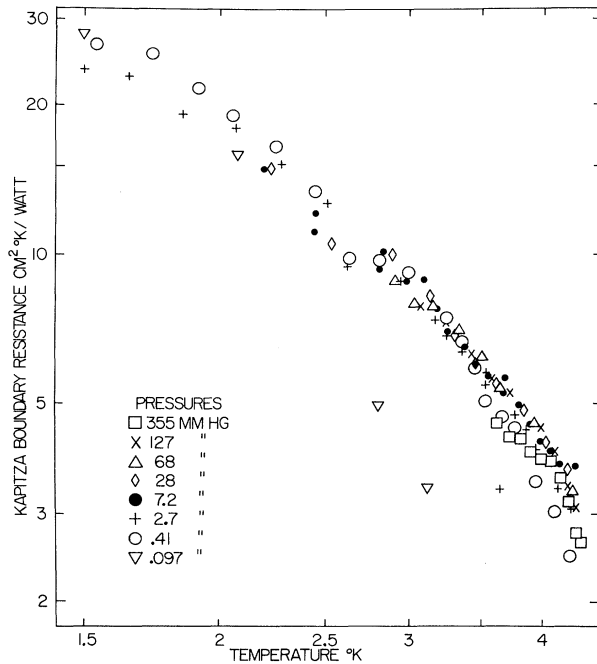


FIG. 3. Kapitza resistance between ^4He gas and a copper surface.

cell width. Between 1.5 and 4°K , the data of Fig. 3 can be represented within the scatter by

$$R(\text{Kapitza}) \simeq 70T^{-2} \text{ }^\circ\text{K cm}^2/\text{W}, \quad (3)$$

which is too fast a temperature dependence to be accounted for by gas conduction. It is perhaps worth noting that an assumption that the cell width has been underestimated by 2.5μ gives a boundary resistance

$$R(\text{Kapitza}) \simeq 85T^{-3} \text{ }^\circ\text{K cm}^2/\text{W}, \quad (4)$$

and that further upward revision of the estimated cell width would drive the boundary-resistance term negative at the higher temperatures. Although large, these boundary resistances are within an order of magnitude of the Kapitza resistances observed between copper and liquid He II,^{1,3,5,8-10} which also fall within the range of temperature dependence embraced by Eqs. (3) and (4). Very similar results have been observed for heat transfer between a solid wall and the mobile helium film.^{11,12}

We conclude that the dominant heat-transfer mechanism at a solid boundary is the same for gaseous helium, both above and below the lambda temperature, as for liquid helium II, and that the energy transfer must therefore

be mediated by helium atoms adsorbed at the solid surface.

*Work supported in part by the National Science Foundation.

¹P. L. Kapitza, J. Phys. (USSR) **4**, 181 (1941).

²W. A. Little, Can. J. Phys. **37**, 334 (1959).

³L. J. Challis, K. Dransfeld, and J. Wilks, Proc. Roy. Soc. (London), Ser. A **260**, 31 (1961).

⁴I. M. Khalatnikov, Zh. Eksperim. i Teor. Fiz. **22**, 687 (1952).

⁵R. C. Johnson and W. A. Little, Phys. Rev. **130**, 596 (1963).

⁶E. H. Kennard, *Kinetic Theory of Gases* (McGraw-Hill Book Company, Inc., New York, 1938), p. 314.

⁷K. Fokkens, W. Vermeer, K. W. Taconis, and R. de Bruyn Ouboter, Physica **30**, 2153 (1964).

⁸D. White, O. D. Gonzales, and H. L. Johnston, Phys. Rev. **89**, 593 (1953).

⁹L. J. Challis, Proc. Phys. Soc. (London) **80**, 759 (1962).

¹⁰K. Wey-Yen, Zh. Eksperim. i Teor. Fiz. **42**, 921 (1962) [translation: Soviet Phys.-JETP **15**, 635 (1962)].

¹¹H. Montgomery and P. A. Matthew, Cryogen. **6**, 94 (1966).

¹²K. Fokkens, K. W. Taconis, and R. de Bruyn Ouboter, Physica **32**, 2129 (1966).

OBSERVATION OF AMPLITUDE OSCILLATIONS OF LARGE-AMPLITUDE ION ACOUSTIC WAVES IN A PLASMA*

Noriyoshi Sato,[†] Hiroyuki Ikezi, Yoshihiko Yamashita,[‡] and Nobuo Takahashi
Institute of Plasma Physics, Nagoya University, Nagoya, Japan

(Received 6 November 1967; revised manuscript received 4 March 1968)

There have been a number of experimental studies¹ on propagation and damping of ion acoustic waves excited externally in a plasma. Since those works were all restricted to small-amplitude waves, the linearized theories² were tested experimentally. On the other hand, in the recent study of Malmberg and Wharton³ on large-amplitude electron plasma waves, amplitude oscillations were observed as predicted by the nonlinear theory.⁴ This Letter reports experimental results on amplitude oscillations of large-amplitude ion acoustic waves excited externally in a thermally ionized cesium plasma.

The plasma ($\sim 3 \times 10^9 \text{ cm}^{-3}$), about 2 cm diam and 130 cm long, is produced by surface ionization of cesium atoms on a tantalum plate heated up to about 2300°K and is confined by an external magnetic field.⁵ The electron temperature is about 2 times larger than the ion temperature. The background gas pressure is $(1-5) \times 10^{-6}$ Torr. Two grids 4 cm diam made of 0.1-mm-diam molybdenum wires spaced 1.5 mm apart are used for wave excitation and detection. The grids, with their planes normal to the axis of the machine, are kept at equal negative bias ($-V_b$) with respect to the hot plate, and are axially movable. Continuous sinusoidal signals ($V_{ex} = 1-50 \text{ V}$ peak to peak, $f = 10-150 \text{ kc/sec}$) are applied to the exciting grid, which varies the transmission rate to the plasma from 5 to 90%. Signals picked up by the receiving grid are fed to a phase-sensitive de-

tector, together with the reference signals from the exciting source. Phase velocity and wave amplitude are obtained from the output plotted on a recorder as a function of the grid separation.

The excited waves propagate along the plasma column and are damped out before reaching the plasma-column end, without any reflection back to the plasma. For small-amplitude waves ($V_{ex} \lesssim$ a few volts peak to peak), the wave

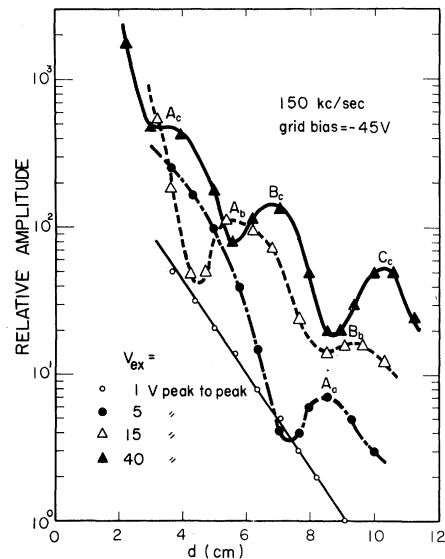


FIG. 1. Relative wave amplitude as a function of the grid separation (d) for various amplitudes of the exciting signal (V_{ex}).